Synchronization transition of identical phase oscillators in a directed small-world network

Ralf Tönjes,[1] Naoki Masuda,[2,3] and Hiroshi Kori[1,3]
[1]Ochadai Academic Production, Ochanomizu University, Tokyo 112-8610, Japan
[2]Graduate School of Information Science and Technology, The University of Tokyo, Tokyo 113-8656, Japan
[3]PRESTO, Japan Science and Technology Agency, Kawaguchi, Saitama 332-0012, Japan

(Received 9 March 2010; accepted 16 July 2010; published online 11 August 2010)

We numerically study a directed small-world network consisting of attractively coupled, identical phase oscillators. While complete synchronization is always stable, it is not always reachable from random initial conditions. Depending on the shortcut density and on the asymmetry of the phase coupling function, there exists a regime of persistent chaotic dynamics. By increasing the density of shortcuts or decreasing the asymmetry of the phase coupling function, we observe a discontinuous transition in the ability of the system to synchronize. Using a control technique, we identify the bifurcation scenario of the order parameter. We also discuss the relation between dynamics and topology and remark on the similarity of the synchronization transition to directed percolation.
 [doi:10.1063/1.3476316]

The adjustment of phase and frequency in large systems of oscillatory units can lead to global coherent oscillations, i.e., synchronization. On the other hand, noise and heterogeneity in the system can weaken synchronization, or even destroy it. Synchronization in the nervous system can facilitate the transfer of information or cause epileptic seizures. Multistability and hysteresis of normal and pathological collective behavior are observed. When all oscillators are identical and the coupling tends to decrease phase differences a state of complete synchronization is asymptotically stable. But even in random networks with uncorrelated and homogeneously distributed node degrees this absorbing state may not be reached or disappear when it is perturbed locally. Here we perform a detailed numerical analysis of the transition between different states of synchronization in a directed small-world network of phase oscillators. By varying the mean in-degree of the network or the nonlinearity of the phase coupling function at zero phase difference, we find discontinuous and continuous transitions with mean field critical behavior.

I. INTRODUCTION

Synchronization in spatially extended systems and complex networks is an important mechanism to create global spatiotemporal correlations from local interaction rules.[1–4] Its applications range from information transfer,[5] self-organized optimization of work flow or traffic flow[6] to the realization of strong coherent oscillations in arrays of Josephson junctions or coupled fiber lasers.[7] The transition to partial synchronization, i.e., the emergence of a nonzero mean field, in systems of nonidentical oscillators is well-known. It has been studied analytically in the original texts by Kuramoto[4,8] and in a more general way in recent papers.[9–11] Recently it has been shown that degree heterogeneity in scale-free random networks of identical oscillators can also lead to desynchronization or partially synchronized states even though complete synchronization is asymptotically stable.[12]

Here we study the transitions from incoherence to partial synchronization and to complete synchronization in a sparse, directed small-world network of identical phase oscillators. Since the formulation of the model,[13] small-world networks have been studied as a medium for dynamical processes, such as the spreading of epidemics,[14] the Ising model,[15–17] and also synchronization of nonidentical phase oscillators.[18] Nontrivial behavior in sparse networks of coupled dynamical systems is known to occur in Boolean networks[19,20] and has also been reported for leaky integrate-and-fire models with and without delay coupling.[21,22] We show, for the case of attractively coupled, identical phase oscillators, that even if the in-degree distribution is homogeneous the system may enter a quasistationary chaotic state of incoherence or partial synchronization. So far, desynchronization, due to inherent heterogeneity, could be analytically described by global and local mean field approaches,[4,9,12] which assume a sufficiently large number of neighbors. In contrast, our model is highly homogeneous, in terms of degree distribution and correlations, and none of the previously described mechanisms for desynchronization in networks of oscillators can explain the observed transition.

II. THE MODEL

The phase dynamics of N identical, weakly coupled limit-cycle oscillators may be described by the Kuramoto phase equations.[2,4,8] In a corotating frame of reference where the common oscillator frequency is zero, these are

$$\dot{\vartheta}_i = \sum_{j=1}^{N} H_{ij} g(\vartheta_j - \vartheta_i), \tag{1}$$

where $H_{ij} \geq 0$ is the coupling matrix and $g(\vartheta_j - \vartheta_i)$ is the coupling function. The coupling function only depends on

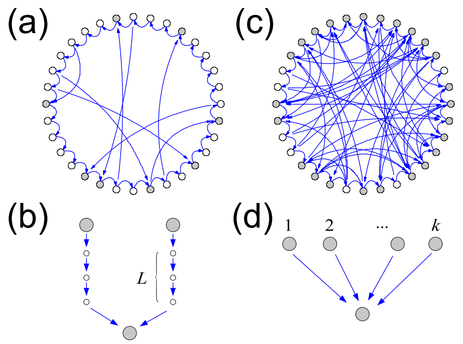

FIG. 1. (Color online) The network model. Unidirectional small-world networks with $N=32$ nodes at [(a) and (b)] low shortcut density $\sigma=0.25$ and [(c) and (d)] higher shortcut density $\sigma=2.0$. Joints of the network, i.e., nodes that receive more than one input, are marked gray. (b) At low shortcut densities most joints couple indirectly to two other joints through linear chain segments of length $L\approx 1/\sigma$. (d) At high shortcut densities each joint couples to $k=\sigma+1$ neighbors which are also with high probability joints.

the phase difference between the oscillators and its shape is characteristic for given coupled limit-cycle oscillators.[4] A typical coupling function, which is, for example, realized in diffusive coupling, has the properties $g(0)=0$ and $g'(0)>0$, implying that the coupling force between two coupled oscillators is attracting and vanishes when they have identical phases. For weakly anharmonic oscillators the coupling function is usually well-approximated by the first harmonics (see, e.g., Ref. 23), i.e.,

$$g(\Delta\vartheta)=\sin(\Delta\vartheta-\alpha)+\sin(\alpha). \tag{2}$$

The parameter α $(-\pi/2<\alpha<\pi/2)$ breaks the antisymmetry of the coupling function around zero, which can lead to nontrivial effects.[4,12,24–26] We can restrict ourselves to non-negative values of α $(0\leq\alpha<\pi/2)$ since a transformation $\alpha\to-\alpha$ and $\vartheta_i\to-\vartheta_i$ for all i leaves Eqs. (1) and (2) invariant.

Under very general conditions, i.e., non-negative coupling strengths $H_{ij}\geq 0$ and a nondegenerate zero eigenvalue of the coupling Laplacian, complete synchronization with $\vartheta_i=\vartheta_j$ for all oscillators i and j is an asymptotically stable solution of Eq. (1).[27] Strong connectedness of the network is a sufficient condition for this. Failure of a system of identical phase oscillators to synchronize cannot be deduced from a local stability analysis of the completely synchronized state. It is the result of a chaotic phase dynamics that riddles the phase space so that complete synchronization cannot be reached.

As a coupling network, we employ a well-established modification[14,21,28] of the original Watts–Strogatz model.[13] Starting with a ring of N unidirectionally coupled oscillators we add N_{sc} unidirectional shortcuts with random origin i and destination j (see Fig. 1). We refer to nodes which receive more than one input as the joints of the network. In addition to the system parameter α, which characterizes the phase coupling function, the shortcut density $\sigma=N_{sc}/N$ characterizes the topology of the coupling network.

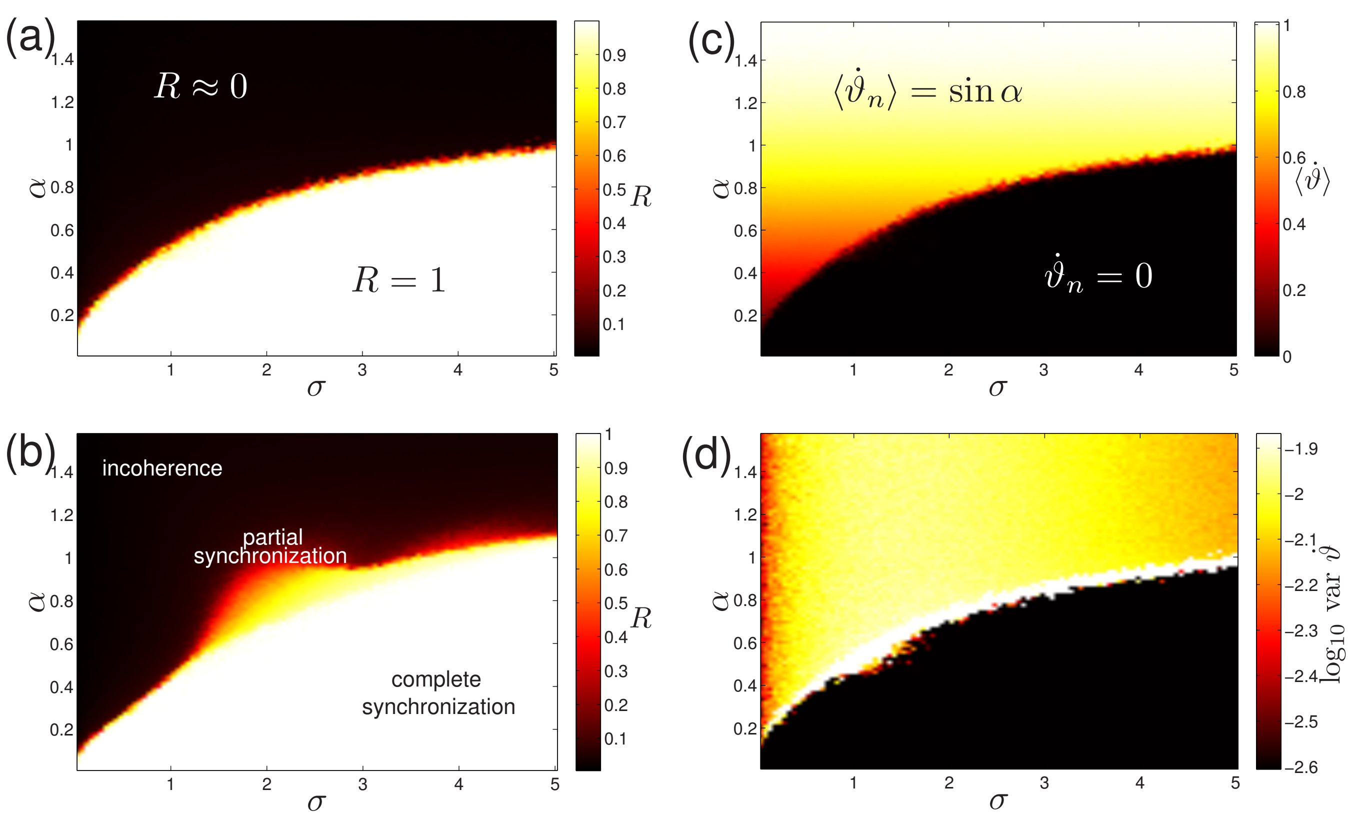

FIG. 2. (Color online) Synchronization transition in the (σ,α) parameter plane. Each point corresponds to an ensemble average over ten network realizations ($N=800$) and time average over 600 units after an initial transient of 200. Shown are (a) the mean order parameter R, (c) the mean oscillator frequency, and (d) the variance of phase velocities in the case of normalized input strength. For comparison we also show (b) the mean order parameter for non-normalized coupling strength for which a larger area of partial synchronization is observed at intermediate shortcut densities.

In the present paper, except for Fig. 2(b), we assume uniform and normalized input strength, i.e.,

$$\sum_{j=1}^{N} H_{ij} = 1 \tag{3}$$

for each oscillator and $H_{ij}=1/k_i^{\mathrm{in}}$ if oscillator i with in-degree k_i^{in} couples to j or $H_{ij}=0$ otherwise. The normalization would have a great impact on the dynamics if the coupling network was very heterogeneous. In the non-normalized case and when the phases are uniformly distributed the phase velocity of each oscillator is biased proportional to its in-degree and $\sin\alpha$.[12] Oscillators with larger in-degree tend to move faster so that degree heterogeneity indirectly leads to a heterogeneity in frequencies. In contrast, when the coupling strength is normalized to unity the bias to the phase velocity is equal to $\sin\alpha$ for all oscillators [see Fig. 2(c)]. However, the directed small-world network model that we use has a Poissonian degree distribution, and is thus a homogeneous network. In fact, we observe similar synchronization behavior with and without the normalization given by Eq. (3) [see Figs. 2(a) and 2(b)]. Another consequence of this normalization is that the phase velocities are bounded, i.e., $-1 \le \dot{\vartheta}_i - \sin\alpha \le 1$ and an oscillator that receives only a single input is always phase locked to it. Phase slips do not occur in a chain of unidirectionally coupled phase oscillators but only at the joints of a network.

III. SIMULATION RESULTS

Figure 2 shows the phase diagrams obtained from numerical integrations of Eq. (1) for networks of $N=800$ oscillators starting from uniformly random initial conditions. For each set of parameter values for σ and α, we show time and ensemble averages of various quantities. Numerical simulations of an ensemble of ten network realizations were run for $T=800$ where an initial transient time of 200 time units was disregarded. In Figs. 2(a) and 2(b), the average order parameter $R=\langle r(t)\rangle_{\mathrm{time,trials}}$, where $r(t)=|\frac{1}{N}\Sigma_i e^{i\vartheta_i(t)}|$ is displayed. Note that $r(t)=1$ for complete synchronization and $R\sim O(1/\sqrt{N})$ for complete incoherence, i.e., uniform phase distribution. There exists a clear transition from an incoherent regime ($R\approx 0$) at small shortcut densities σ or larger asymmetry α to a coherent regime ($R=1$) at higher shortcut density or lower asymmetry. To quantify the dynamical properties of the incoherent state, we also observed the mean frequency $\langle \dot{\vartheta}_i(t)\rangle_{i,\mathrm{time,trials}}$ [Fig. 2(c)] and the variance of the phase velocities, $\langle \mathrm{var}\ \dot{\vartheta}_i(t)\rangle_{i\ \mathrm{time,trials}}$ [Fig. 2(d)].

Figure 3(b) shows the distribution of phase velocities, which is characteristic for the phase diffusion process in the incoherent state. The variance of the phase velocities is a measure for the internal noise due to chaotic phase dynamics. We observe that the mean frequency in the incoherent state with normalized input strength is equal to $\sin\alpha$ independent of σ, while the variance of the phase velocities is independent of α.

Figure 4 shows snapshots of the first 200 phases in a network of $N=1000$ oscillators. In the incoherent state for low σ [Fig. 4(a)], the one-dimensional chain segments sustain traveling waves with an average phase difference of α between neighboring oscillators. Forward and backward phase slips occur occasionally in the joints of the network when the phase of the local mean field changes rapidly as it passes the vicinity of zero. In the partially synchronized state for low σ [Fig. 4(b)], the phases of the chain segments evolve around a global mean field. When a forward slip between the phase of a joint and the global mean field occurs, all oscillators in the chain segment adjacent to this joint will also perform a phase slip at a delayed time. For a high shortcut density no spatial patterns exist [Figs. 4(c) and 4(d)].

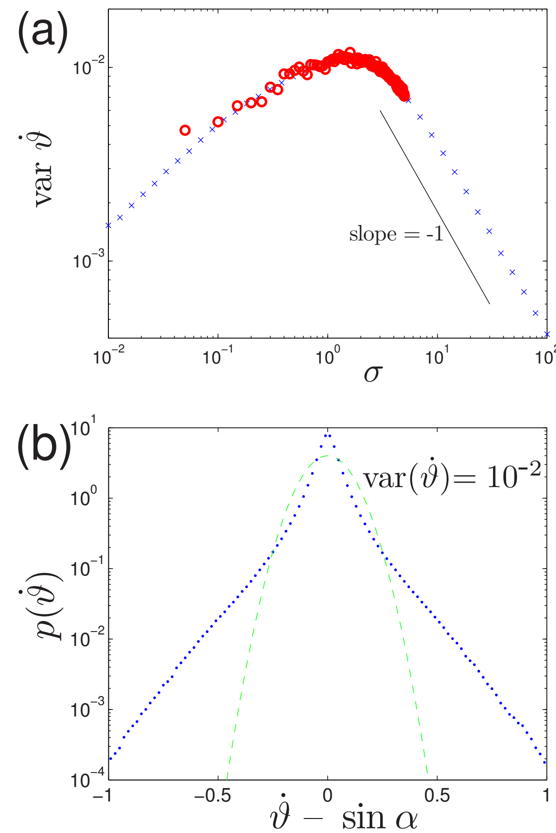

FIG. 3. (Color online) Variance and distribution of phase velocities in the incoherent state. (a) Variance of phase velocities obtained from simulations with $N+N_{\mathrm{sc}}=10^6$ and $\alpha=\pi/2$ (crosses) and from the simulations presented in Fig. 2(d) (circles) at $\alpha=1.2$. (b) The distribution of phase velocities in the incoherent state at $\sigma=1.0$ (dots) is centered around the mean of $\langle\dot{\vartheta}\rangle=\sin\alpha$. It is peaked at the center and much broader than a Gaussian distribution of the same variance (dashed line).

A. Control scheme and bifurcation scenario

A more detailed examination using a linear control scheme reveals the bifurcation scenario for the order parameter. Assuming that the order parameter $r(t)$ evolves according to some unknown mean field dynamics, we make the ansatz

$$\dot{r} = f(r,\alpha,\sigma,\eta(t)), \tag{4}$$

where $\eta(t)$ represents intrinsic or external noise. In the absence of noise the dynamics under the general linear control scheme

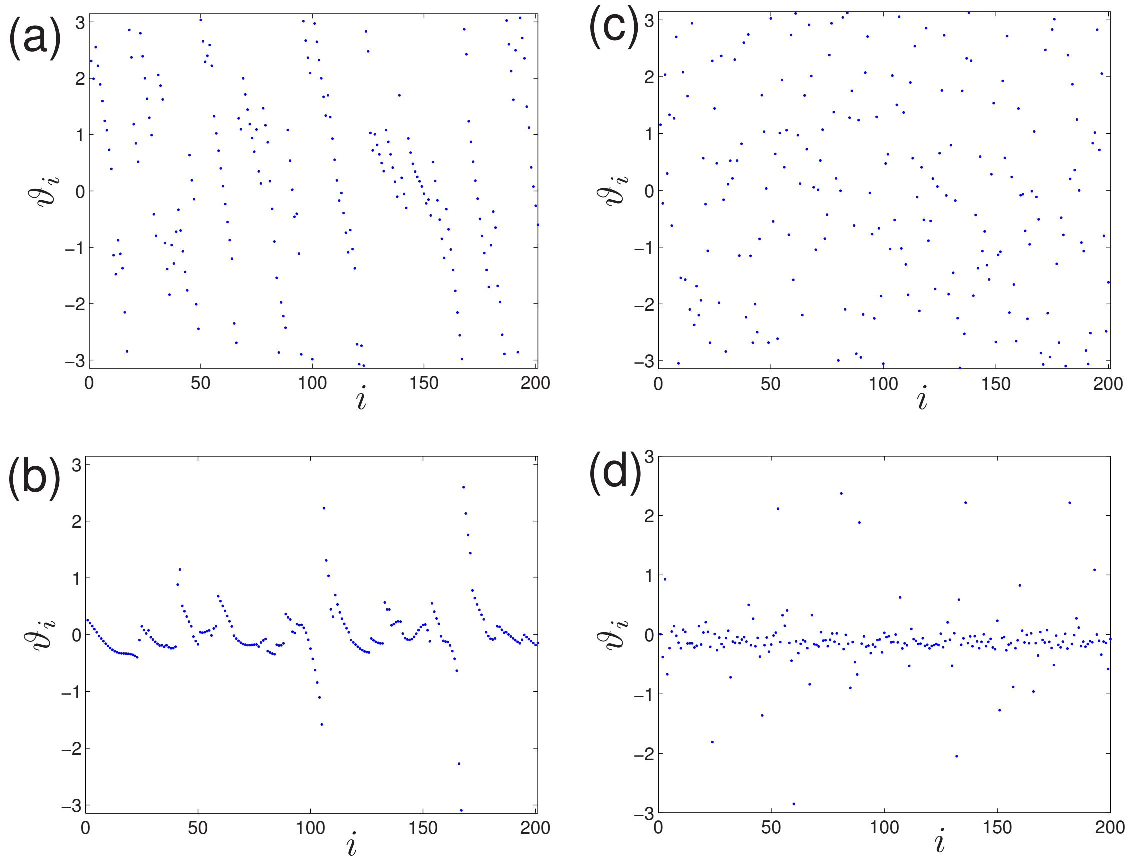

FIG. 4. (Color online) Snapshots of the first 200 phases in a system of $N=1000$ oscillators in a dynamical (quasi) equilibrium state for low shortcut density $\sigma=0.35$ ($\alpha=0.36$) in (a) and (b) and high shortcut density $\sigma=128$ ($\alpha=1.5$) in (c) and (d). (a) and (c) show the stable incoherent state in a parameter region of bistability with the partially synchronized states shown in (b) and (d). Only at low shortcut densities the phases have a spatiotemporal structure at the length scale $1/\sigma$ of the chain segments.

$$\dot{\alpha} = c_0(r - r_0) + c_1\dot{r} \tag{5}$$

has the fixed point $r=r_0$ and $\alpha=\alpha_0(r_0,\sigma)$ with $\dot{r}=f(r_0,\alpha_0,\sigma,0)=0$. In Appendix B we show that, in the absence of noise, sufficiently large positive values of c_0 and c_1 can stabilize any fixed point r_0. In the presence of noise, the time derivative of r may not be well-defined. We thus use a short-time average of r and $\dot{r}$ instead of their instantaneous values, i.e.,

$$\dot{\alpha} = c_0(\langle r(t)\rangle_\gamma - r_0) + c_1\langle \dot{r}(t)\rangle_\gamma, \tag{6}$$

where

$$\langle r(t)\rangle_\gamma = \gamma\int_0^\infty r(t-\tau)e^{-\gamma\tau}d\tau \tag{7}$$

and

$$\langle \dot{r}(t)\rangle_\gamma = \gamma\int_0^\infty \dot{r}(t-\tau)e^{-\gamma\tau}d\tau$$

are interpreted as stochastic integrals.

Using the control scheme given by Eq. (6), and appropriately tuned parameters γ, c_0, and c_1, we succeeded to trace the stable and unstable branches in the bifurcation diagram of r as a function of the control parameter α at fixed shortcut densities σ (Fig. 5). We find that the incoherent state always loses stability in a discontinuous transition at a critical value $\alpha_{\mathrm{HP}}(\sigma)$. We conjecture that this transition is a subcritical Hopf bifurcation of the complex mean field. The branch of unstable partially synchronized states may fold back and become stable in a saddle-node bifurcation at a parameter $\alpha_{\mathrm{SN}}(\sigma)$. This hysteresis behavior is most pronounced around $\sigma\approx 1$ with possibly small parameter regions in which multiple partially synchronized states are stable [Fig. 5(c)]. At α_{P} the branches of partial synchronization connect to the absorbing state of complete synchronization with $r=1$. In the next section (Sec. III B) we perform a finite size scaling analysis at this transition point and conclude that it is of mean field directed percolation universality. From these simulations, we could determine the three curves $\alpha_{\mathrm{HP}}(\sigma)$, $\alpha_{\mathrm{SN}}(\sigma)$, and $\alpha_{\mathrm{P}}(\sigma)$ for a large range of shortcut densities (Fig. 6).

B. Nonequilibrium transition to complete synchronization

In finite systems, the partially synchronized state may disappear after a long transient time, and the state of complete synchronization is approached at an exponential rate. This sudden change of behavior resembles the transition from an active state to the absorbing state in directed percolation processes.[29]

Finite size scaling analysis in low-dimensional coupling topologies has demonstrated that synchronization in coupled

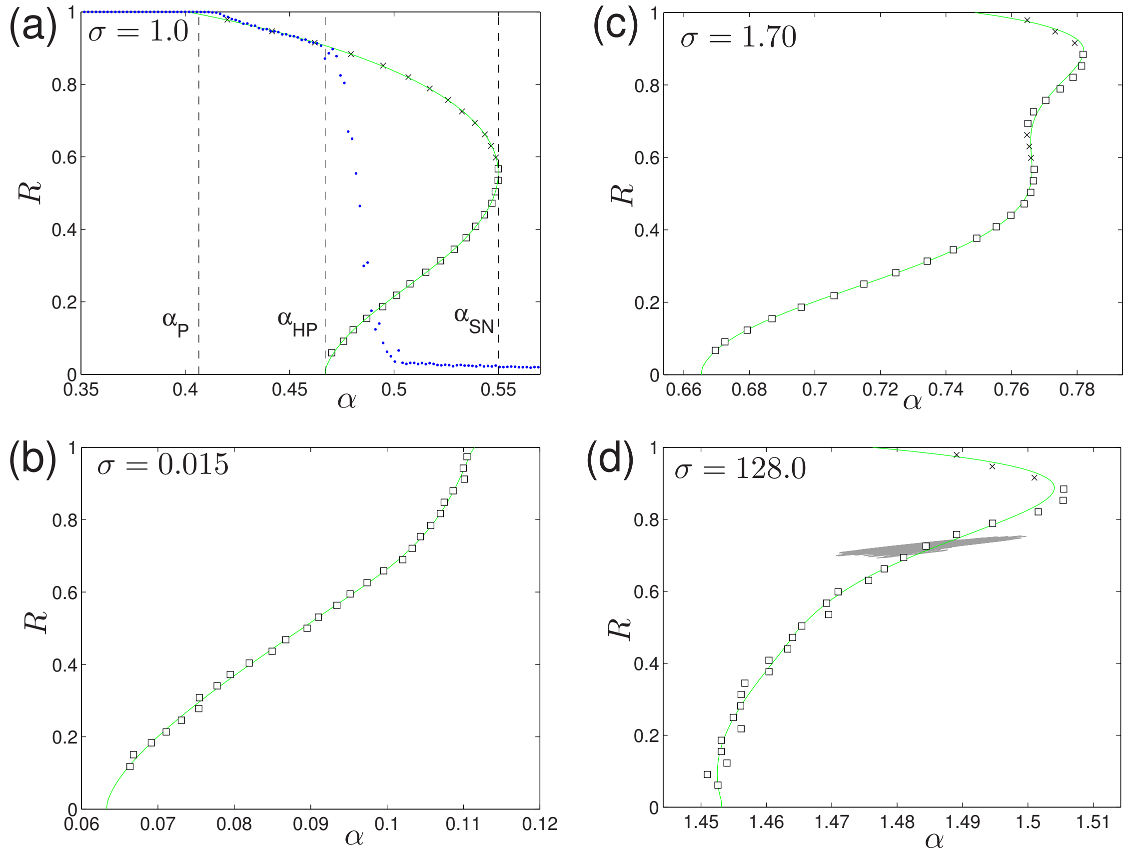

FIG. 5. (Color online) Bifurcation diagram of the order parameter R as a function of control parameter α at selected values of shortcut densities σ. Points on the branches of unstable (open squares) and stable (crosses) partially synchronized states were obtained as averages of the trajectory (R,α) [see light gray area in (d)] under the control scheme given by Eq. (6). The green lines are sixth order polynomial fits $\alpha(R)$ constrained to $\alpha'(0)=0$ because of the assumption of a Hopf bifurcation of the incoherent state. From these fits we also find the threshold $\alpha_{\mathrm{P}}=\alpha(1)$ for complete synchronization and the points of saddle node bifurcations α_{SN} of stable and unstable partially synchronized states. The dots in (a) are the average order parameter in simulation with networks of $N=8000$ oscillators. Each point is an ensemble average of the order parameter over 50 realizations after 1000 units of time.

map lattices is of Kardar–Parisi–Zhang or directed percolation universality.[30] In a small world network, the transition is expected to be of mean field universality.[15,18]

To examine this point we have performed a finite size scaling analysis in the vicinity of α_{P} at fixed shortcut density $\sigma=1.0$. The initial condition was a stable partially synchronized state at $\alpha=0.52$ and $R\approx 0.75$. After a transient time we decreased α and observed how $r(t)$ approached zero. From simulation runs with single realizations of networks with sizes up to $N=10^6$ oscillators in the vicinity of the transition point, we found $\alpha_{\mathrm{P}}=0.4065$ and $(1-R)\sim(\alpha-\alpha_{\mathrm{P}})^{\beta}$ with $\beta=1.01$ (Fig. 7). This exponent is consistent with mean field universality of directed percolation. The nonequilibrium nature of the phase transition is expressed in the time dependence of the probability distribution of the order parameter. In a finite directed percolation system with a unique absorbing state, this absorbing state will be reached with probability one after a long enough transient time, even when a stable nonzero mean field solution exists.[31]

A suitable absorbing state for a network of coupled phase oscillators can be defined via a Lyapunov function. Let $V:[0,2\pi]^N \to [0,2\pi]$ denote the minimal length of the arc that contains the phases of all oscillators. Then one can show that V is a Lyapunov function in any subset B_S of the phase space with $V(B_S)\leq \pi-2\alpha$. If the network is strongly connected, i.e., there exists a directed path between any two nodes, and $H_{ij}\geq 0$ then one can show that $\dot{V}<0$ for all $V>0$ in B_S. Thus B_S defines an absorbing state in which complete synchronization, i.e., $V=0$, is approached exponentially.

Let $\mu(\alpha,N,t)$ denote the probability of a process to have reached the absorbing state prior to the time t, then the finite size scaling ansatz for this probability is

$$\mu(\alpha,N,t)=\tilde{\mu}((\alpha-\alpha_{\mathrm{P}})N^{\nu},N^{-z}t). \tag{8}$$

This probability can be determined by averaging over a large number of simulation runs. At each value of α in Fig. 7(c) we have performed 100 simulations for system sizes $1000 \leq N \leq 64\,000$. To determine the exponent z we have performed 1000 simulation runs for each system size at the critical parameters $\alpha=\alpha_{\mathrm{P}}=0.4065$ and $\sigma=1.0$. At the transition point the median $T_{1/2}$ defined as $\mu(\alpha,N,T_{1/2})=0.5$ scales with the system size as

$$T_{1/2}(N)\sim N^{z}. \tag{9}$$

The third critical exponent ν is related to the width and the position of the transition. Defining the position of the transition as $\mu(\alpha_{1/2},N,N^{z}T_0)=0.5$ one finds

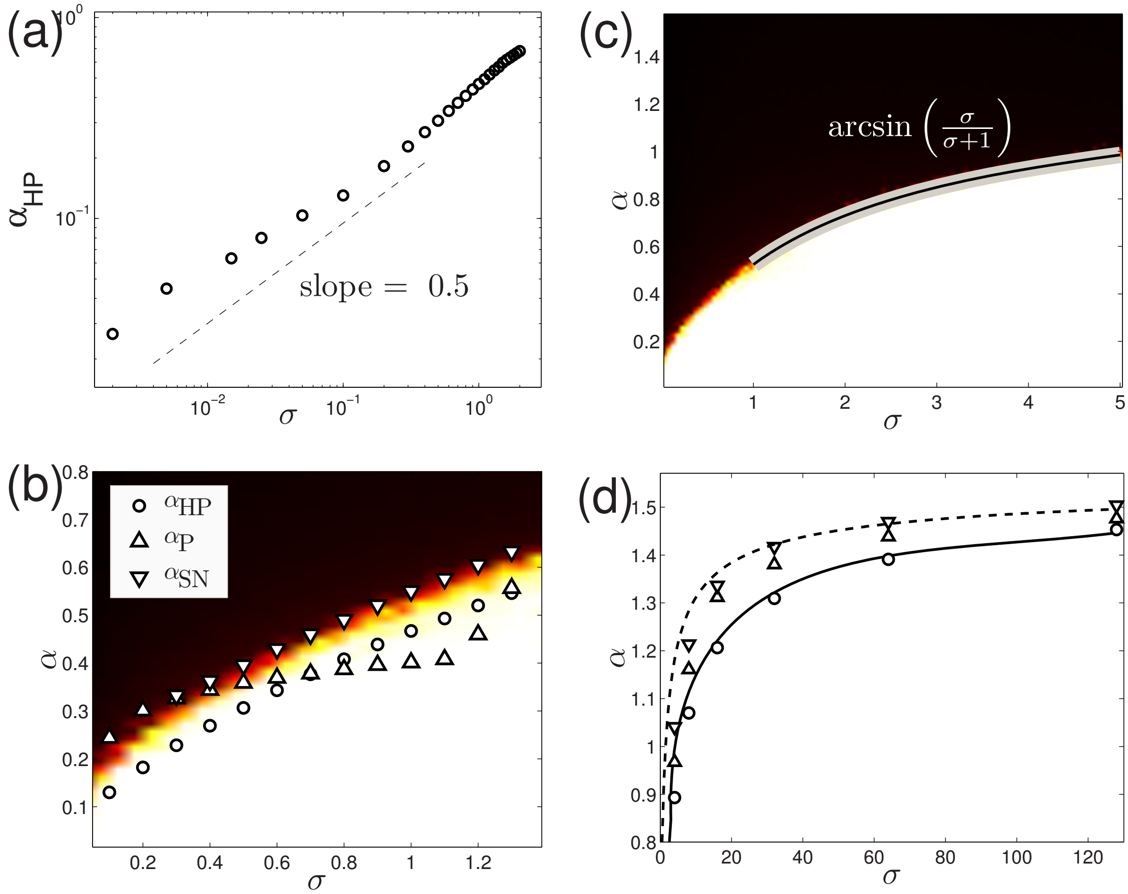

FIG. 6. (Color online) Numerically determined synchronization points for (a) low shortcut densities, [(b) and (c)] intermediate shortcut densities, and (d) large shortcut densities. The open circles and the upward and the downward triangles mark the Hopf bifurcation points $\alpha_{HP}(\sigma)$ of the incoherent state, the transition points $\alpha_P(\sigma)$ to complete synchronization, and the saddle-node bifurcation points $\alpha_{SN}(\sigma)$, respectively. Stable partial synchronization is found between $\alpha_P(\sigma)$ and $\alpha_{SN}(\sigma)$. At intermediate to large shortcut densities [(c) and (d)] the transition to synchronization is very well-described by $\alpha_{HP}(\sigma)=\arcsin(\sigma/(\sigma+1))$ (solid line). This is not the case for very low shortcut densities (a) where $\alpha_{HP}(\sigma)$ approaches zero more slowly than linearly. The line of slope 0.5 in the double-logarithmic plot (a) is drawn for comparison. The critical line $\alpha_{HP}(\sigma)=\arccos(0.85/\sqrt{\sigma+1})$ obtained from the heuristic mean field ansatz equation (13) [dashed line in (d)] agrees qualitatively with the asymptotic approach of α_{HP} to $\pi/2$ but is larger than the values obtained by our control scheme (open circles). The color code for the background of (b) and (c) is the same as in Figs. 2(a) and 2(b).

$$(\alpha_{1/2}-\alpha_P) \sim N^{-\nu}. \tag{10}$$

Confidence intervals for the experimentally determined values of z and ν could be estimated by bootstrapping on the sample of simulation runs. However, we presume that systematic errors are dominating for the relatively small system sizes used in our simulations leading to slightly higher values of z and ν than the expected value of 0.5 for mean field directed percolation. We find $z\approx 0.54$ and $\nu\approx 0.55$.

IV. DISCUSSION

So far, we have presented our numerical results. In this section, we discuss the different dynamical regimes of our model and the mechanism for desynchronization.

A. Topological crossover

Our small-world network model exhibits a topological crossover between low shortcut densities $\sigma<1$ and high shortcut densities $\sigma>1$. The two regimes are characterized by the scaling of the average distance between successive joints of the network, which are oscillators that couple to more than one neighbor, along an arbitrary path (see Fig. 1). By choosing the end points of the shortcuts randomly and uncorrelated, the number L of nodes between two joints on the original ring lattice is exponentially distributed as $p(L)\sim\exp(-\sigma L)$ in the limit $N\to\infty$. The expected value of L is $\langle L\rangle=(\exp(\sigma)-1)^{-1}$, which is approximately σ^{-1} at low shortcut densities and $\exp(-\sigma)$ at high shortcut densities. This crossover is reflected in the phase dynamics of the incoherent state as a regime of traveling waves on the original ring lattice at $\sigma<1$ to a regime without clear spatiotemporal patterns at $\sigma>1$ (Fig. 4).

The Poissonian degree distribution with a mean in-degree of $k=\sigma+1$ and standard deviation $\sqrt{k}$ provides homogeneity at high shortcut densities. On the other hand, at low shortcut densities $\sigma<1$, the network consists of one-dimensional chain segments which interact nonlinearly at the joints of the network. The network of joints, where chain segments are replaced by edges and indirect interactions, is also very homogeneous, since the number of joints which receive exactly two inputs is of order $O(\sigma)$ while the total number of all other joints is of order $O(\sigma^2)$. In this sense, the network is most inhomogeneous at intermediate shortcut densities $\sigma\approx 1$ where the amount of short chain segments

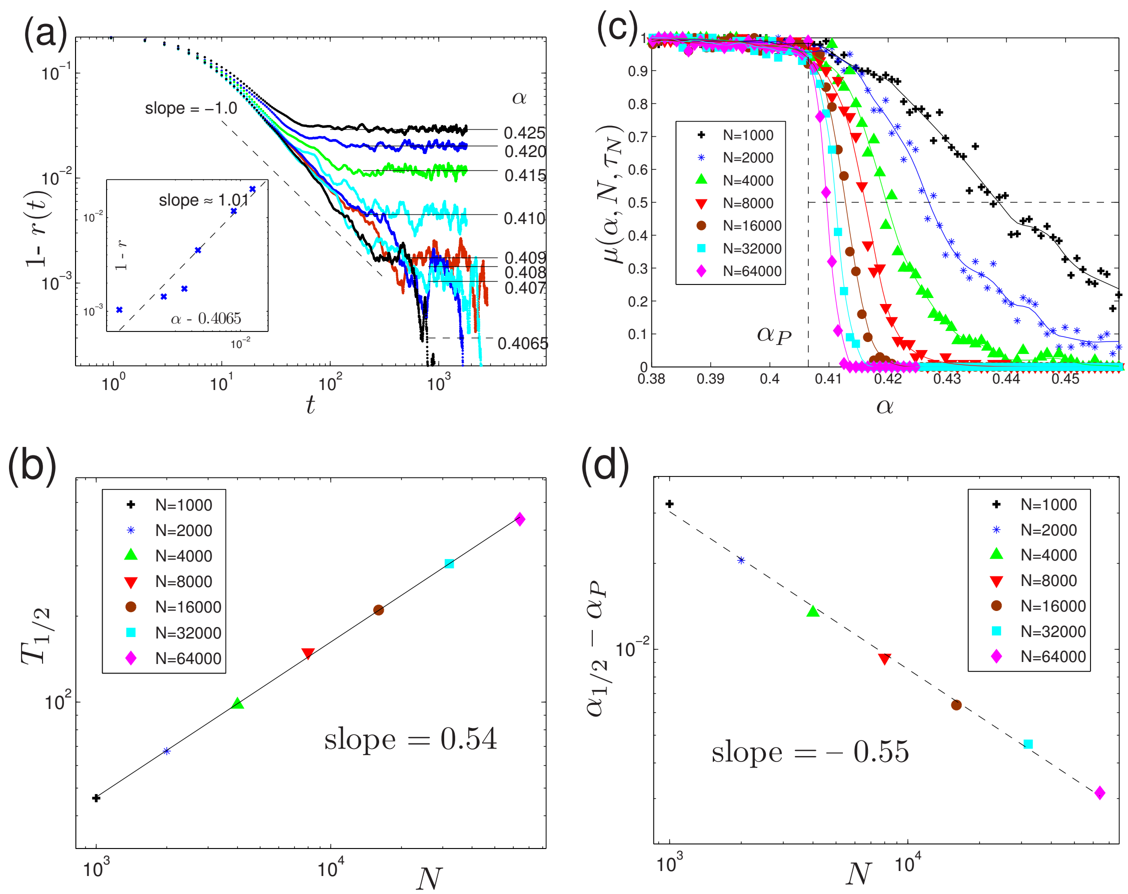

FIG. 7. (Color online) Finite size scaling analysis of the nonequilibrium transition from partial to complete synchronization at α_P for $\sigma=1.0$. In (a) simulation runs with system sizes up to $N=10^6$ were performed. At the critical point complete synchronization merges with the metastable partially synchronized state which is approached as t^{-1} if the transition is of mean field directed percolation universality. The line $(1-r(t)) \sim t^{-1}$ is drawn for comparison. The inset shows the linear approach of the mean order parameter $r \rightarrow 1$ in the vicinity of the critical point. The line of slope 1.01 is a linear fit to the data in double-logarithmic scales. Other critical exponents are obtained from the time statistics for a realization to reach the absorbing state of complete synchronization. (b) shows the median of this time at the critical point for various system sizes. In (c) we plot the fraction μ_0 of 100 realizations which reach complete synchronization before the time $\tau_N=1900(N/64\,000)^{0.54}$ for different N as a function of α. This defines a median $\alpha_{1/2}$, shown in (d), which approaches the critical point $\alpha_P=0.4065$ at a power law with exponent of -0.55 as a function of N.

and joints with more than two input links is comparable. Indeed, this topological complexity is reflected in a maximum of the variance of the phase velocities at intermediate shortcut densities, which quantifies the strength of the internal noise (see Fig. 3). We will discuss the dynamical properties of our model for low and high shortcut densities, separately.

B. Statistical properties of the incoherent state

In the incoherent state, the phases undergo a chaotic phase diffusion process. An oscillator coupled to a finite number of neighbors is therefore subject to a fluctuating force. In the incoherent state in a unidirectional network, the neighbors of an oscillator have independent phases, because their distance is of the order of the network diameter. Thus, if the number of neighbors k is sufficiently large, the local mean fields will fluctuate around zero with approximately Gaussian distribution and one can show that its variance is equal to k^{-1}. Since the amplitudes of the local mean fields determine the phase velocities of the oscillators which in turn generate the local mean fields, the chaotic phase diffusion process is invariant under a rescaling of time as $k^{-1/2}$ (see Appendix A for details). From the circular autocorrelation function $c(\tau)=\langle\cos(\vartheta(t+\tau)-\vartheta(t))\rangle$ we can estimate the effective phase diffusion constant D and an effective scattering rate γ of the chaotic phase diffusion process by comparing it directly to the autocorrelation function of a Brownian flight on the circle[32] with

$$c(\tau) = e^{-D\tau+D\gamma^{-1}(1-e^{-\gamma\tau})}. \tag{11}$$

The variance of the phase velocities of such a Brownian flight is equal to $v^2=D\gamma$ and can directly be compared to the variance $\mathrm{var}(\dot{\vartheta})$ of the chaotic phase diffusion process. In Table I we show the experimentally determined effective diffusion constant and the variance of the phase velocities for $k=25$, 64, and 100, and $\alpha=\pi/2$. We find the predicted scaling of D, γ, and $\mathrm{var}(\dot{\vartheta})$. In particular the rescaled effective phase diffusion constant is $D\sqrt{k}\approx 0.13$.

Note that these statistical properties do not depend on α, as can be seen in Fig. 2.

TABLE I. Time scales of the chaotic phase diffusion process for various large mean degrees $k \gg 1$. We find that the effective phase diffusion constant and the effective scattering rate scale with $1/\sqrt{k}$ and the variance of the phase velocities scales as $1/k$ [see Fig. 3(b)]. The transition point to synchronization α_{HP} has been determined with the help of our control scheme.

k	25	64	100
$D\sqrt{k}$	0.1252	0.1296	0.1417
$\gamma\sqrt{k}$	0.4064	0.3937	0.3598
$k\ \mathrm{var}(\dot{\vartheta})$	0.0478	0.0519	0.0544
$kD\gamma = kv^2$	0.0509	0.0510	0.0510
α_{HP}	1.27	1.39	1.43

C. Synchronization transition for high shortcut density

In the incoherent state each oscillator in the network is subject to a fluctuating local mean field generated by a finite number of neighbors performing the chaotic phase diffusion process. These neighbors sample from the global distribution of phases. While the global mean field evolves deterministically in the thermodynamic limit $N \to \infty$, the local mean fields will be approximately distributed as a Gaussian around the global mean field with a variance of order $O(1/k)$, a relaxation rate γ, and a diffusion constant D of order $O(1/\sqrt{k})$. Let us define the complex correlation function

$$c_{ij} = \langle z_i^* z_j \rangle, \tag{12}$$

where $z_j = \exp(i\vartheta_j)$ and the average is over time. In our homogeneous network model, the correlation is a function c_L of the length L of the shortest directed path from j to i. A heuristic mean field ansatz is to use this correlation function as a distance dependent weight and phase shift for the coupling

$$\dot{\vartheta}_i = R \frac{\sum_{L=1}^{\infty} \mathrm{Im}[c_L^* e^{i(\Theta - \vartheta_i)}]}{\sum_{L=1}^{\infty} |c_L|}, \tag{13}$$

where R and Θ are the mean field amplitude and angle. Here we have chosen a corotating reference system where $\langle \dot{\vartheta} \rangle = 0$. In the incoherent state the complex correlation function (Fig. 8) has the form

$$c_L = \varrho^{|L|} e^{iL\alpha} = (\varrho_0 k^{-1/2})^{|L|} e^{iL\alpha}. \tag{14}$$

Each shell, i.e., a set of oscillators j with constant distance L from i, is correlated to the oscillator i with an amplitude that decreases exponentially with L and at an angle which changes linearly with L. The factor ϱ_0 was determined to be

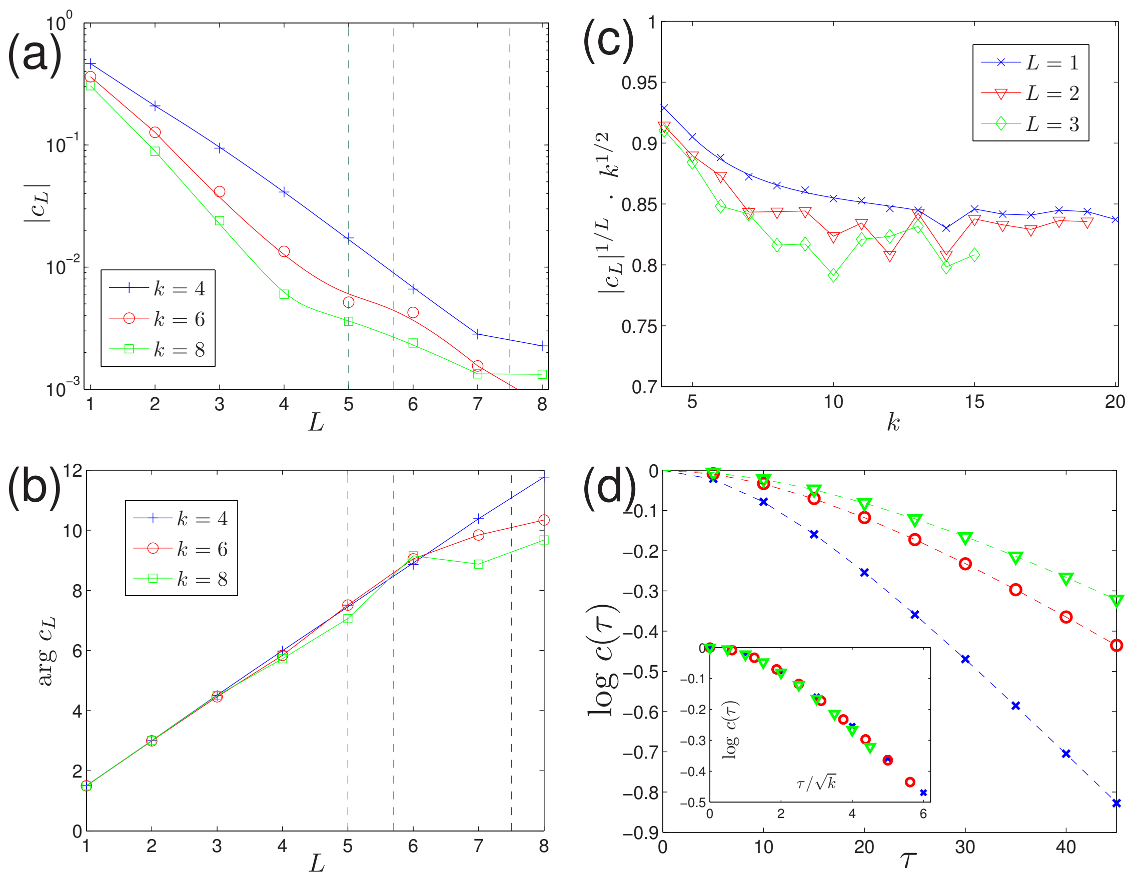

FIG. 8. (Color online) Complex correlation function in the incoherent state. (a) Absolute value in logarithmic scales as a function of the distance L on the ring backbone of the network for $k = \sigma + 1 = 4$ (blue crosses), $k=6$ (red circles), and $k=8$ (green squares). (b) Angle as a function of the distance L on the ring backbone of the network for $k=4$ (blue crosses), $k=6$ (red circles), and $k=8$ (green squares). We used $\alpha = 1.5$, well above the synchronization threshold. The dashed lines in (a) and (b) mark the mean distance $\log N/\log k$ in the network of size $N = 32\,000$. (c) Scaling of absolute value with the number of neighbors at distance $L=1$ (blue crosses), $L=2$ (red triangles), and $L=3$ (green diamonds). (d) Logarithm of autocorrelation function at time difference τ for $k=25$ (blue crosses), $k=64$ (red circles), $k=100$ (green triangles) and parametric fit to autocorrelation function of Brownian flight on the circle [Eq. (11), dashed lines]. See Table I for values of D and γ. The inset shows the collapse of the curves under a rescaling of time with factor $k^{-1/2}$.

approximately 0.85 [see Fig. 8(c)]. We are now able to express the phase evolution as that of a globally coupled system with effective coupling strength κ_{eff} and effective asymmetry $\alpha_{\mathrm{eff}} > \alpha$ as

$$\dot{\vartheta}_i = \kappa_{\mathrm{eff}} R \sin(\Theta - \vartheta_i - \alpha_{\mathrm{eff}}), \tag{15}$$

where κ_{eff} and α_{eff} are determined by

$$\kappa_{\mathrm{eff}} e^{-i\alpha_{\mathrm{eff}}} = \frac{(1-\varrho)}{\varrho} \sum_{L=1}^{\infty} (\varrho e^{-i\alpha})^L = \frac{(1-\varrho)e^{-i\alpha}}{1-\varrho e^{-i\alpha}}. \tag{16}$$

This mean field ansatz predicts a stable incoherent state whenever $\alpha_{\mathrm{eff}} \geq \pi/2$ which is fulfilled if

$$\cos\alpha < \varrho_0 k^{-1/2}. \tag{17}$$

The critical line $\alpha_{\mathrm{HP}} = \arccos(\varrho_0/\sqrt{k})$ obtained from this heuristic mean field ansatz shows the same qualitative behavior as the critical line obtained from the control scheme, although the numerical values do not agree well [see Fig. 6(d)]. It predicts an asymptotic approach of α to $\pi/2$ at the order of $O(1/\sqrt{k})$ as $k \to \infty$.

Another heuristic argument can be made for the transition line $\alpha_{\mathrm{P}}(\sigma)$. Suppose that all oscillators have the same phase $\vartheta_i = 0$ except one oscillator with phase ϑ_0 which is externally driven. This oscillator assumes the role of an active seed in terms of percolation processes. If this active seed activates (i.e., induces oscillations of) the other oscillators that couple to the seed, the whole system may eventually become active, resulting in the incoherent or partially synchronized states. We are thus interested in the conditions under which an oscillator with phase ϑ_1 and in-degree k that couples to the seed can become active. The phase equation for ϑ_1 is initially

$$\dot{\vartheta}_1 = \frac{1}{k}\sin(\vartheta_0 - \vartheta_1 - \alpha) - \frac{k-1}{k}\sin(\vartheta_1 + \alpha) + \sin\alpha. \tag{18}$$

At criticality, we expect that the phase difference $\vartheta_0 - \vartheta_1$ is drifting fast so that the first term of Eq. (18) can be time averaged and neglected. In this case, oscillator 1 gets activated for $(k-1)/k > k-1/k$, and with $k = \sigma + 1$ we obtain the condition

$$\alpha = \arcsin\frac{\sigma}{\sigma+1} \tag{19}$$

for criticality. Equation (19) agrees surprisingly well with the numerically determined transition line $\alpha_{\mathrm{HP}}(\sigma)$ for $\sigma > 1$ but less well with $\alpha_{\mathrm{P}}(\sigma)$ [Figs. 6(c) and 6(d)]. Again we predict that the critical α approaches $\pi/2$ at the order of $O(1/\sqrt{k})$.

D. Synchronization transition for low shortcut density

For low shortcut densities $\sigma < 1$, the situation becomes even more complicated. Due to the topological crossover another length scale σ^{-1} is introduced in the system. The dynamics in the incoherent state for low shortcut densities is characterized by traveling waves along one-dimensional chain segments of the original ring topology which interact nonlinearly at the joints of the network (see Fig. 4). We call the first and last oscillators in a chain segment the head and the tail of the chain, respectively. For normalized input strength the chain segments are always phase locked to the head but act as a low pass filter to the phase dynamics (Appendix C). As a result, the variance of the phase velocities decreases along a chain segment and for smaller values of σ (Fig. 3). The interaction between the joints of the network is indirect and involves delay and additional phase shifts. Also, the correlation between the head and an oscillator down the chain segment decreases exponentially with the distance between the head and the oscillator. These factors seem to inhibit synchronization so that the critical $\alpha_{\mathrm{HP}}(\sigma)$ is still decreasing for $\sigma \ll 1$ but much slower than linearly [Fig. 6(a)].

V. SUMMARY AND CONCLUSIONS

We have shown that a finite average number of neighbors and an asymmetry of the phase coupling function can inhibit synchronization in homogeneous networks of identical oscillators. Using a control technique, we could construct the bifurcation diagram for the order parameter.

A finite size scaling analysis at the nonequilibrium phase transition from partial synchronization to complete synchronization shows critical exponents of mean field universality. In contrast to Ref. 12 it is not the heterogeneity of the node degree distribution that drives the system away from synchronization. Instead, it is the interplay between the spatial structure of the network and the internal noise which prevents the oscillators from reaching synchronization. The temporal fluctuations generated by the system itself in the chaotic incoherent or partially synchronized state give rise to a correlation function that decays exponentially with the distance. Using this correlation function to formulate a heuristic mean field theory for the incoherent state, we have qualitatively explained the transition from incoherence to synchronization.

Our main results are derived from numerical simulations. An analytic description of the transition curve and the chaotic phase diffusion process in the incoherent state remain challenging open problems.

ACKNOWLEDGMENTS

We thank Hugues Chaté and Kazumasa Takeuchi for valuable discussion about directed percolation processes. R.T. acknowledges Professor Yasumasa Nishiura, funding through a JSPS short term fellowship (PE.07606) and by JST Special Coordination Funds for Promoting Science and Technology. N.M. acknowledges the support through the Grants-in-Aid for Scientific Research (Grant Nos. 20760258 and 20540382) from MEXT, Japan.

APPENDIX A: SCALING ARGUMENT FOR $\sigma \gg 1$

Here we will present the details of the scaling argument that relates the amplitude and the time scale of the fluctuations in the local fields. Let us consider the dynamics of the complex state $z_i = \exp(i\vartheta_i)$ of an oscillator

$$\dot{z}_i = i\,\mathrm{Im}[z_i^* \Psi_i e^{-i\alpha}] z_i = r_i i\,\mathrm{Im}[e^{i(\Theta_i - \theta_i - \alpha)}] z_i, \tag{A1}$$

where Ψ_i is the local field given by

$$\Psi_i = \sum_j H_{ij} z_j = r_i e^{i\Theta_i}. \tag{A2}$$

The amplitude and the time scale of local field dynamics can be inferred from the complex correlation function

$$c_\Psi(\tau) = \langle \Psi_i^*(t+\tau)\Psi_i(t)\rangle, \tag{A3}$$

where $\langle \cdots \rangle$ indicates the time average with respect to the stationary processes $z_j(t)$. Assuming k independent neighbors with correlation function

$$c_z(\tau) = \langle z_j^*(t+\tau) z_j(t)\rangle, \tag{A4}$$

one finds exactly

$$c_\Psi(\tau) = \frac{1}{k} c_z(\tau). \tag{A5}$$

This relation is remarkable since it is valid for all k and all time differences τ. Therefore, the phase dynamics of the local fields has exactly the same time scale as the dynamics of the phase oscillators. Without calling on the central limit theorem this relation also gives the mean square amplitude of the local fields as $\langle r^2\rangle = c_\Psi(0) = k^{-1}$ for all k.

The assumption of independent phases of the neighbors only holds in large unidirectional networks in the incoherent state. Due to the chaotic dynamics, correlations between oscillators decay exponentially with the distance in the network which is of order $O(\log N/\log k)$ (Fig. 8).

The effective phase diffusion constant can be defined by the asymptotic behavior of $c_\Psi(\tau)$ and $c_z(\tau)$ at large τ,

$$D = -\lim_{\tau\to\infty} \frac{d}{d\tau} \ln c(\tau). \tag{A6}$$

We recall that the circular autocorrelation function for a free Brownian flight on the circle is $c(\tau) = \exp(-D\tau + D/\gamma(1-\exp(-\gamma\tau)))$, where γ is an effective scattering rate and D is the effective phase diffusion constant.[32] Exponential decay is expected at time scales $\tau\gamma \gg 1$. From Eqs. (A5) and (A6) it follows that the effective phase diffusion constants of the single oscillator phase and that of the local fields are identical. For sufficiently large k, the local fields are normally distributed and it is only the amplitude of the local fields that decreases when k is increased. The process (A1) is therefore invariant under a rescaling

$$t' = \sqrt{\frac{k}{k'}} t, \qquad \Psi'(t') = \sqrt{\frac{k}{k'}} \Psi(t). \tag{A7}$$

In our model, this rescaling is achieved by changing the number of neighbors from k to k'. The second transformation affects both the amplitude and the phase diffusion time scale of the local fields.

Because of the homogeneity of our model, we can assume statistical equivalence of the phase dynamics for all oscillators. The phase $\vartheta_i(t)$ of an oscillator that is coupled via Eq. (A1) to k independent but identically distributed phase diffusion processes $\vartheta_j(t)$ must be another realization of the same process. In particular, the effective phase diffusion constant must be the same. To get insight into the phase diffusion process, let us examine an oscillator with complex state z that is coupled to a complex Ornstein–Uhlenbeck process Ψ,

$$\dot\Psi = -D\Psi + \sqrt{D}\eta, \qquad \dot z = iz\,\mathrm{Im}[z^*\Psi], \tag{A8}$$

where η is complex Gaussian white noise of unit strength in real and imaginary part. Note that the Ornstein–Uhlenbeck process Ψ is only an approximation of the dynamics of an actual local field which has the same Gaussian stationary distribution with expected square amplitude $\langle r^2\rangle = 1$. The effective phase diffusion constant as defined in Eqs. (A3) and (A6) is $D_\Psi = D$.[32] The effective phase diffusion constant D_z depends nonlinearly on D_Ψ. For large values of D the time scales of Ψ and z are separated and the phase of z will diffuse much slower than the phase of Ψ. For very small values of D the phase of z will almost always be locked to the phase of Ψ. Only when Ψ diffuses near zero, phase slips may occur which add a ballistic component to the evolution of z and can increase the effective phase diffusion constant D_z to a value larger than D.

There exists a fixed point D^* for which the time scales of Ψ and z are identical. The fixed point D^* should be close to the actual value of the self-consistent solution. A self-consistent solution must also yield Eq. (A5). The average field of k such processes z may be normally distributed but is not an Ornstein–Uhlenbeck process. However, the iterative procedure of coupling a phase oscillator to k independent neighbors defines a mapping in the space of stationary processes on the circle. Starting with a Brownian phase diffusion we see that in the first iteration the map is contracting with respect to the effective diffusion constant (Fig. 9), an

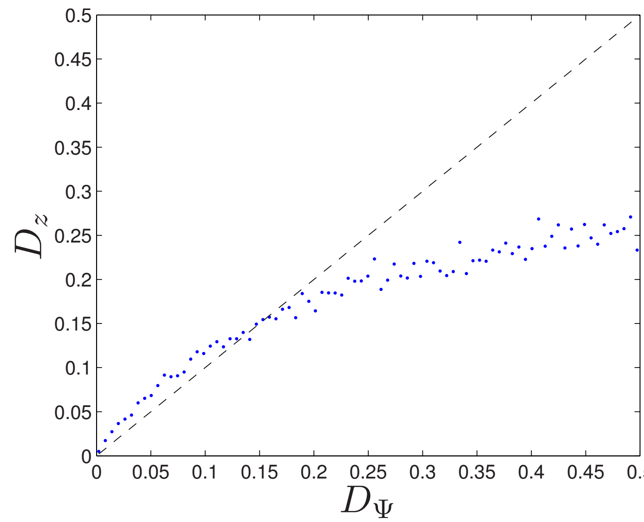

FIG. 9. (Color online) Effective phase diffusion constant D_z of a phase oscillator with complex state variable z coupled to a complex valued Ornstein–Uhlenbeck process of unit variance and phase diffusion constant D_Ψ [Eq. (A8)]. The fixed point at $D^* \approx 0.15$ is expected to be close to the rescaled effective phase diffusion constant $D(k)\sqrt{k}$ of the characteristic stationary phase diffusion process in the incoherent state for $k \gg 1$.

indication for the existence of a unique stationary phase diffusion process characterizing the incoherent state.

We have measured D_z as a function of D in numerical integration of Eq. (A8) and found the fixed point to be $D^* \approx 0.15$. Table I shows the effective diffusion constants in our model for $k=25$, 64, and 100, obtained from a nonlinear parametric least squares fit to the autocorrelation function (system average). We find that $D\sqrt{k}\approx 0.13$ agrees well with this value.

APPENDIX B: CONTROL SCHEME

Given the mean field dynamics

$$\dot{r} = f(r,\alpha) \tag{B1}$$

of a scalar order parameter r with a system parameter α, we are interested in the bifurcation curve $\alpha_0(r)$ with $f(r,\alpha_0(r))=0$. If we can control the system parameter $\alpha=\alpha(t)$ then the linear control scheme

$$\dot{\alpha} = c_0(r-r_0) + c_1\dot{r} \tag{B2}$$

has the fixed point $(r,\alpha)=(r_0,\alpha_0(r_0))$. With $f_0=\partial_r f(r_0,\alpha_0(r_0))$ and $f_1=\partial_\alpha f(r_0,\alpha_0(r_0))$ the Jacobian of the combined mean field and control dynamics reads

$$J = \begin{pmatrix} f_0 & f_1 \\ c_0 & c_1 f_1 \end{pmatrix}. \tag{B3}$$

Assuming $f_1<0$, the conditions for stability $\mathrm{tr}(J)<0$ and $\mathrm{Det}(J)>0$ yield

$$c_1 > -\frac{f_0}{f_1} \quad \text{and} \quad c_0 > f_0 c_1. \tag{B4}$$

The assumption of $f_1<0$ applies, since an increase of α counteracts synchronization and decreases r if $\alpha>\alpha_0(r)$. Sufficient conditions to stabilize any point $(r_0,\alpha_0(r_0))$, regardless of the sign of f_0, i.e., of the stability of the uncontrolled fixed point, are

$$c_0 > |f_0| c_1 > \frac{f_0^2}{|f_1|}. \tag{B5}$$

APPENDIX C: THE OVERDAMPED LINEAR CHAIN

For low shortcut densities one can view the dynamics in the small-world network as traveling waves which interact through a network of joints. Each joint of the network is the head of a unidirectional chain segment. A joint receives input from at least two nodes of other chain segments. To understand the role of the chain segments in the transition to synchronization, we study the dynamics of the phases and the signal transmission along a chain segment in a linear approximation.

The phase equations for a unidirectionally coupled chain of oscillators are

$$\dot{\vartheta}_n = \sin(\vartheta_{n-1} - \vartheta_n - \alpha) + \sin\alpha. \tag{C1}$$

We identify ϑ_0 with the phase in the head oscillator of the chain and ϑ_L with the phase of the tail oscillator. Under appropriate boundary conditions Eq. (C1) allows for traveling wave solutions $\dot{\vartheta}=\sin\alpha$ and $\vartheta_{n-1}-\vartheta_n=\alpha$. In principle, all frequencies in the interval $[\sin\alpha-1, \ \sin\alpha+1]$ and corresponding phase differences are possible but we choose the traveling wave solution with the average frequency $\sin\alpha$. Small deviations x_n from this solution can be studied in a linear approximation

$$\dot{x}_n = x_{n-1} - x_n, \tag{C2}$$

which can be solved given the trajectory $x_0(t)$ in the head of the chain. The system is asymptotically independent from initial conditions and the solution is

$$\begin{aligned} x_n(t) &= \int_0^\infty e^{-\tau} x_{n-1}(t-\tau)\,d\tau \\ &= \int_0^\infty \tau^{n-1}\frac{e^{-\tau}}{(n-1)!} x_0(t-\tau)\,d\tau. \end{aligned} \tag{C3}$$

The dynamics in the tail of a chain is a time convolution of the dynamics in the head of the same chain around the traveling wave solution. A discontinuous jump of the phase in the head of the chain will translate at unit speed while the width of the phase jump grows at the same rate, as a result of the gamma distribution for the time convolution kernel. In this linear approximation, the deviation from the traveling wave solution grows diffusively with the distance from the head of the chain. Suppose the head of the chain performs a Brownian motion with $\langle (x_0(t)-x_0(0))^2\rangle = 2Dt$. Then we obtain

$$\langle (x_n(t)-x_0(t))^2\rangle = \langle x_n(t)^2\rangle_{x_0(t)=0}, \tag{C4}$$

and

$$\begin{aligned} \langle x_n(t)^2\rangle_{x_0(t)=0} &= \langle x_n(0)^2\rangle_{x_0(0)=0} \\ &= \int_0^\infty dT dT' \frac{(TT')^{n-1}e^{-(T+T')}}{\Gamma^2(n)} \\ &\quad \times \langle x_0(-T)x_0(-T')\rangle_{|x_0(0)=0} \\ &= 2\int_0^\infty dT d\tau \frac{(T(T+\tau))^{n-1}e^{-T}e^{-(T+\tau)}}{\Gamma^2(n)} \\ &\quad \times \langle x_0^2(-T)\rangle_{|x_0(0)=0} \\ &= 4D\int_0^\infty dT \frac{T^n e^{-T}}{\Gamma(n)}\frac{\Gamma(n,T)}{\Gamma(n)}. \end{aligned} \tag{C5}$$

Using

$$\Gamma(n+1,T) = n\Gamma(n,T) + T^n e^{-T} \tag{C6}$$

we obtain

$$\langle x_n^2(0)\rangle_{|x_0(0)=0} = 4D\int_0^\infty dT \frac{T^n e^{-T}}{\Gamma(n+1)}\frac{n}{\Gamma(n+1)} \times(\Gamma(n+1,T) - T^n e^{-T})$$
$$= 2Dn\left(1-2\int_0^\infty \frac{T^{2n}e^{-2T}}{\Gamma^2(n+1)}\right)$$
$$= 2Dn\left(1-\frac{\Gamma(2n+1)}{\Gamma^2(n+1)}4^{-n}\right)$$
$$\approx 2Dn\left(1-\frac{1}{\sqrt{n\pi}}\right). \quad \text{(C7)}$$

The effective spatial phase diffusion constant along a linear chain of oscillators is the same as the temporal diffusion constant of the phase in the head of the chain. The complex correlation function

$$c_{L0}(0) = \langle z_L^*(t) z_0(t)\rangle \sim e^{i\alpha L - DL} \quad \text{for} \quad L \gg 1 \quad \text{(C8)}$$

has an amplitude that decreases exponentially with the chain length. A lower shortcut density therefore decreases the correlation between the joints of the network, making it more difficult to synchronize.

[1]G. V. Osipov, J. Kurths, and C. Zhou, *Synchronization in Oscillatory Networks*, Springer Series in Synergetics (Springer, Berlin, 2007).
[2]A. Pikovsky, M. Rosenblum, and J. Kurths, *Synchronization : A Universal Concept in Nonlinear Sciences*, Cambridge Nonlinear Science Series Vol. 12 (Cambridge University Press, Cambridge, England, 2001).
[3]A. T. Winfree, *The Geometry of Biological Time*, Interdisciplinary Applied Mathematics Vol. 12, 2nd ed. (Springer-Verlag, New York, 2001).
[4]Y. Kuramoto, *Chemical Oscillations, Waves, and Turbulence*, Springer Series in Synergetics Vol. 19 (Springer-Verlag, Berlin, 1984).
[5]A. Díaz-Guilera and A. Arenas, *Bio-Inspired Computing and Communication* (Springer-Verlag, Berlin, 2008), p. 184.
[6]S. Lämmer, H. Kori, K. Peters, and D. Helbing, Physica A **363**, 39 (2006).
[7]M. Silber, L. Fabiny, and K. Wiesenfeld, J. Opt. Soc. Am. B **10**, 1121 (1993).
[8]Y. Kuramoto, *International Symposium on Mathematical Problems in Theoretical Physics*, Kyoto University, Kyoto, 1975, Lecture Notes in Physics Vol. 39 (Springer, Berlin, 1975), pp. 420–422.
[9]J. G. Restrepo, E. Ott, and B. R. Hunt, Phys. Rev. E **71**, 036151 (2005).
[10]E. Ott and T. M. Antonsen, Chaos **18**, 6 (2008).
[11]A. Pikovsky and M. Rosenblum, Physica D **238**, 27 (2009).
[12]T.-W. Ko and G. B. Ermentrout, Phys. Rev. E **78**, 026210 (2008).
[13]D. J. Watts and S. H. Strogatz, Nature (London) **393**, 440 (1998).
[14]M. E. J. Newman and D. J. Watts, Phys. Rev. E **60**, 7332 (1999).
[15]M. Ostilli and J. F. F. Mendes, Phys. Rev. E **78**, 031102 (2008).
[16]A. Barrat and M. Weigt, Eur. Phys. J. B **13**, 547 (2000).
[17]S. N. Dorogovtsev, A. V. Goltsev, and J. F. F. Mendes, Phys. Rev. E **66**, 016104 (2002).
[18]H. Hong, M. Y. Choi, and B. J. Kim, Phys. Rev. E **65**, 026139 (2002).
[19]B. Derrida and Y. Pomeau, EPL **1**, 45 (1986).
[20]K. Klemm and S. Bornholdt, Phys. Rev. E **72**, 055101 (2005).
[21]A. Roxin, H. Riecke, and S. A. Solla, Phys. Rev. Lett. **92**, 198101 (2004).
[22]S. Jahnke, R.-M. Memmesheimer, and M. Timme, Phys. Rev. Lett. **100**, 048102 (2008).
[23]I. Z. Kiss, Y. Zhai, and J. L. Hudson, Phys. Rev. Lett. **94**, 248301 (2005).
[24]B. Blasius and R. Tönjes, Phys. Rev. Lett. **95**, 084101 (2005).
[25]Y. Kuramoto and D. Battogtokh, Nonlinear Phenom. Complex Syst. **5**, 380 (2002).
[26]D. M. Abrams and S. H. Strogatz, Phys. Rev. Lett. **93**, 174102 (2004).
[27]R. Tönjes and B. Blasius, Phys. Rev. E **80**, 026202 (2009).
[28]M. Barahona and L. M. Pecora, Phys. Rev. Lett. **89**, 054101 (2002).
[29]H. Hinrichsen, Adv. Phys. **49**, 815 (2000).
[30]V. Ahlers and A. Pikovsky, Phys. Rev. Lett. **88**, 254101 (2002).
[31]B. Gaveau and L. S. Schulman, J. Stat. Phys. **70**, 613 (1993).
[32]H. Risken, *The Fokker-Planck Equation, Methods of Solution and Applications*, Springer Series in Synergetics Vol. 18, 2nd ed. (Springer-Verlag, Berlin, 1989).